

Residual Lignocellulosic Biomass-based Activated Biochar: Comparison Between Single and Two-step Thermochemical and Activation Processes

Eriz Corro, Mirari Antxustegi, Julen Murua Berrio, Maria Gonzalez Alriols *

Biorefinery Processes Research Group (BioRP), Chemical and Environmental Engineering Department, University of the Basque Country (UPV/EHU), Avda. Otaola 29, 20600, Eibar, Spain
maria.gonzalez@ehu.eus

Lignocellulosic biochar has become a research hotspot recently due to its versatility in several applications for environmental remediation. It is a sustainable material, which has been proven to offer high performance in applications such as effluent treatment (through the adsorption of organic and inorganic compounds), CO₂ capture, air cleaning or silage agent. Typically, a chemical activation is applied to biochars after the thermochemical process, to increase the porosity of this solid in terms of active surface area as well as pore size and distribution, to improve its performance as adsorbent. Activation with KOH has been proved to achieve well developed pore structure and active functional groups on the biochar surface. Excellent adsorption results for the removal of different pollutants have been reported with biochars produced by the mentioned method. Focusing on a potential scale and industrialization of the lignocellulosic biochar production process, the combination of the thermochemical and chemical activation processes in one step could be interesting in terms of simplicity and time saving. In this work, activated biochars were prepared using a lignocellulosic agricultural waste (apple pruning) as precursor and KOH as a chemical activator, by two different processes: a single and a two-step route, to compare the properties of the biochars generated by both processes. The obtained materials were characterized in terms of proximal analysis, active surface area, pore size and pore distribution. Furthermore, adsorption capacity ABCs was tested and compared.

1. Introduction

The use of heavy metals and synthetic dyes in several industrial activities and its harmful consequences for the environment and human health has been the focus on numerous research efforts with the aim of finding effective solutions for the remediation of wastewater (Sun and Wang, 2023). Lignocellulosic biochar, a carbon-rich substrate obtained by thermochemical conversion of lignocellulosic biomass, has positioned high as adsorbent for the treatment of water effluents due to its advantages, such as world-wide availability, low cost, large specific surface area, well-distributed pores, and strong interaction between the functional groups (Gallego-Ramírez et al., 2022). Research in the field of biochar is progressing non-stop in the last decade, covering aspects such as the used raw material, experimental processing conditions (heating rate, temperature, pressure), biochar physical-chemical properties, or its applications. Extensive review works have been published summarizing the influence of the type of substrate and processing technology on the yield and performance of the obtained biochars (Liu et al., 2023). Focusing on biochar's adsorption properties, its surface and pore accessibility are enhanced by physical or chemical activation. The latter is more efficient than physical one reaching larger surface areas and a more developed porous structure in a faster process with lower activation temperatures (Hui and Zaini, 2015). Usually, chemical activation is performed in a double-step route, the substrate is firstly submitted to a pyrolysis process and the generated biochar is then impregnated with a chemical product and then submitted again to a second thermochemical step for its activation (Oginni et al., 2019). The applied chemical agent significantly influences the characteristics of the resulting activated carbon.

Activation with KOH has been proved to achieve well developed pore structure and active functional groups on the biochar surface (Lü et al., 2022) Excellent adsorption results for the removal of different pollutants have been reported with biochars produced by pyrolysis followed by KOH activation, in a two-step process (Jedynak and Charmas, 2023). In this route, the pre-carbonization makes the biochar more susceptible to chemical reaction with KOH, which leads to larger specific surface area and the formation of a higher degree of mesopores and micropores. Nevertheless, yields associated to the two-step route are typically low (around 12-20%) so, following the current research interest oriented to advance in the upscale of experiments from laboratory conditions to industrial ones, it is of great significance to increase the competitiveness of the biochar production process (Chen et al., 2022). That means to design an efficient route for biochar production at industrial scale, in terms of product yield, time, energy and chemicals consumptions (Luo et al., 2022). The one step process consists of the impregnation of the precursor with the chemical product and the application of a subsequent thermochemical process to the impregnated carbon source. The use of a one-step technology combining the thermochemical and chemical activation treatments in one step process could be interesting in terms of simplicity and time saving. Therefore, in this work, apple pruning (a lignocellulosic waste) as precursor and KOH as chemical activator were used for the obtaining of activated biochar by a single and a two-step routes. The resulting carbonaceous materials (activated apple pruning biochar-1step, APBC-1S and two-step, APBC-2S) were characterised and its performance as adsorbents of an organic dye (methylene blue) from an aqueous stream was compared with the aim of evaluating the impact of the biochar obtaining route.

2. Materials and methods

Apple tree pruning (AP) provided from local suppliers was the selected lignocellulosic biomass substrate for this work. Proximate and ultimate analysis of the raw material as well as of the obtained biochar samples was done following the standards and equipment indicated in a previous publication (Antxustegi et al., 2022). The microscopic structure and morphology of the samples were examined by Scanning Electron Microscopy (SEM) using a JEOL JSM-7000F microscope. The available functional groups on each material surface were analysed by Attenuated Total Reflection-Fourier Transformed Infrared Spectroscopy (ATR-FTIR) using a Perking Elmer Spectrum Two Spectrometer equipped with a Universal Attenuated Total Reflectance accessory provided with an internal reflection diamond crystal. The spectra were collected in the 4000-600 cm^{-1} range with 4 cm^{-1} resolution and 20 scans per spectrum in transmission mode. The textural properties (specific surface area, micropore volume and average pore width) of carbon materials were determined by gas adsorption/desorption experiments. Nitrogen isotherms (-196 °C) were collected in a Micrometrics ASAP 2010 after outgassing the sample under vacuum at 150 °C overnight. Adsorption-desorption and pore size distribution curves were obtained applying the non-local density functional theory (NLDFT).

2.1 One and two-step routes definition

Pyrolysis and activation procedures for the two-step route were done following a previously optimized experimental route (Antxustegi et al., 2022). Experimental conditions of the one-step route were: AP was impregnated with the activation agent (KOH) in a 1/3 wt. ratio. Then, they were introduced to the tubular furnace under N_2 atmosphere (20L/min continuous flow), at a heating rate of 20K/min up to 900°C, reaction time at 900°C: 2 h. Samples were subsequently washed using the same method and the 2 step samples (Antxustegi et al., 2022).

2.2 Adsorption experiments

Adsorption tests were carried following an optimized experimental procedure (Martelo et al., 2022).

3. Results

Table 1 presents the results in terms of proximate and ultimate analyses of samples. O/C indexes for APBC-1S and APBC-2S were 0.17 and 0.33. O/C index is typically calculated as an indirect measurement of aromaticity because the sample's carbon percentage increases as the thermochemical treatment goes by due to dehydration and depolymerization reactions as well as volatilization, eventually leading to the formation of H and O depleted aromatic C structures (Wang et al., 2013). Thus, the one-step route led to biochar samples with higher percentages of carbon, as the total thermochemical treatment was considerable shorter than the one of the 2-step route. The proportion of aromatic rings increases with temperature and residence time at the highest temperature. In fact, the longer residence times of the pyrolysis process the higher carbon percentage as char in the samples at the same heating temperature. Furthermore, H is also lost during condensation of aromatic structures at high temperatures so, H/C index values probably indicates both an increasing number of aromatic rings and an increasingly condensed nature of the aromatic rings (Wiedemeier et al., 2015).

Table 1: Proximate and ultimate analysis, (dry basis, wt. %) of apple tree pruning (AP) and the obtained activated bio-chars from one (APBC-1S) and two-step (APBC-2S) routes.

Parameter		AP	APBC-1S	APBC-2S
Proximate analysis (wt.%)	Fixed carbon (%)	14.86	-	-
	Volatile matter (%)	79.69	-	-
	Inorganic matter (%)	5.45	-	-
	Moisture (%)	8.68	-	-
Ultimate analysis (wt.%, ash free)	C (%)	45.04	85.05	74.87
	H (%)	5.71	-	-
	N (%)	0.73	0.40	-
	S (%)	0.72	0.11	0.48
	O* (%)	42.35	14.44	24.65

* O was calculated by difference.

3.1 Characterization of adsorbents

Morphology of activated biochar samples was analysed by scanning electron microscopy (SEM) and the obtained images corresponding to APBC-1S and APBC-2S are presented in Figure 1.

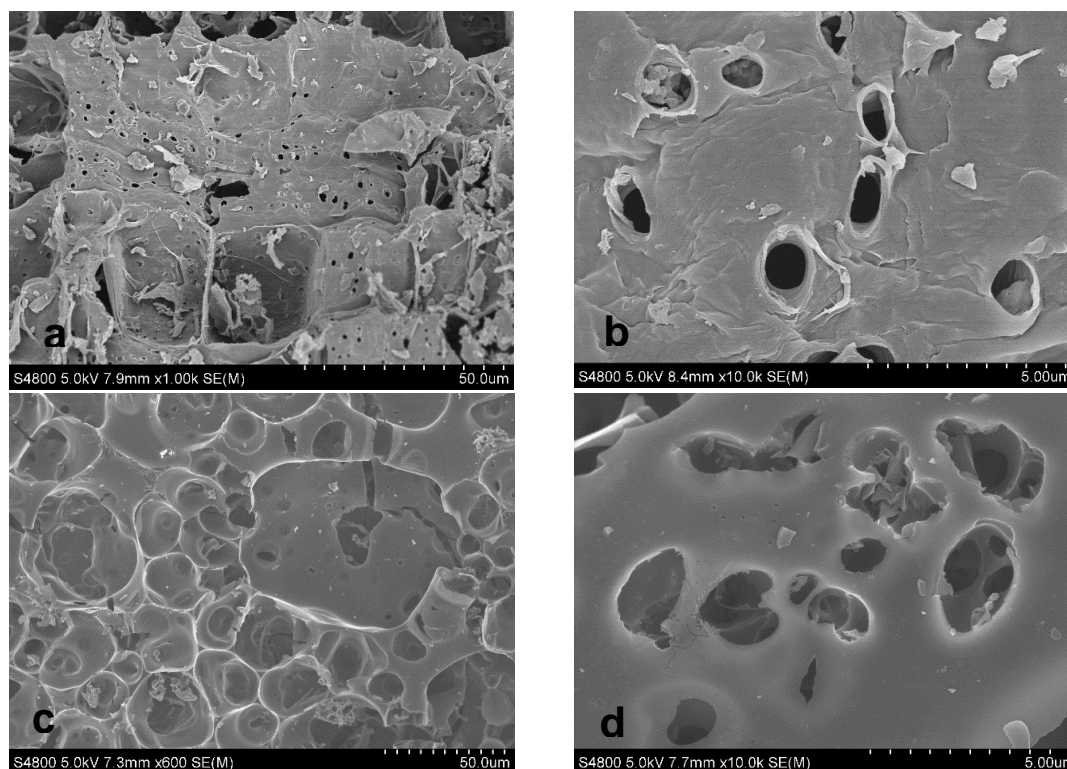


Figure 1: SEM images of APBC-1S (a, b) and APBC-2S (c, d).

The morphology of both samples' surfaces is different, with smaller pore sizes and a rougher surface texture in APBC-2S sample, in which some of the AP original structure of irregular polyhedral cells was partially conserved. On the contrary, APBC-1S sample presented a flat surface with no texture, maybe related to the more explosive treatment performed in the simultaneous pyrolysis and chemical activation.

The Attenuated Total Reflection-Fourier Transformed Infrared Spectroscopy (ATR-FTIR) spectra of AP biomass (Figure 2) revealed transmittance bands of functional group characteristics of lignocellulosic materials, including cellulose, hemicellulose, and lignin. Thus, the most prominent peaks in the spectrum were originated from -OH stretching vibration (3350 cm^{-1}) and C-O (primary alcohols), C=C and C-O-C stretching symmetric stretching vibrations (1042 cm^{-1}). The peak at 1421 cm^{-1} is attributed to the skeletal vibration of the aromatic ring in lignin carbon, and peaks at 1234 and 1108 cm^{-1} corresponded to C-O stretching vibration and the aromatic C-H stretching in guaiacyl units of lignin. In addition, the heterogeneity of functional groups and, consequently, of components on the surface of the material was demonstrated by the high number of sharp

peaks between 1100-1800 cm^{-1} (Kundu et al., 2023). Some of the peaks around 1600 cm^{-1} (aromatic C=C stretching in lignin), 1450 cm^{-1} (C-H deformation in lignin and carbohydrates), 1230 cm^{-1} (C-O stretching in lignin), 1040 cm^{-1} (C-O stretching of carboxylic, ester and ether groups in cellulose and hemicelluloses), clearly visible in AP spectra, could be found in APBC-2S one but not so much in APBC-1S spectra, evidencing differences in the abundancy of chemical groups of both biochars (Siipola et al., 2018).

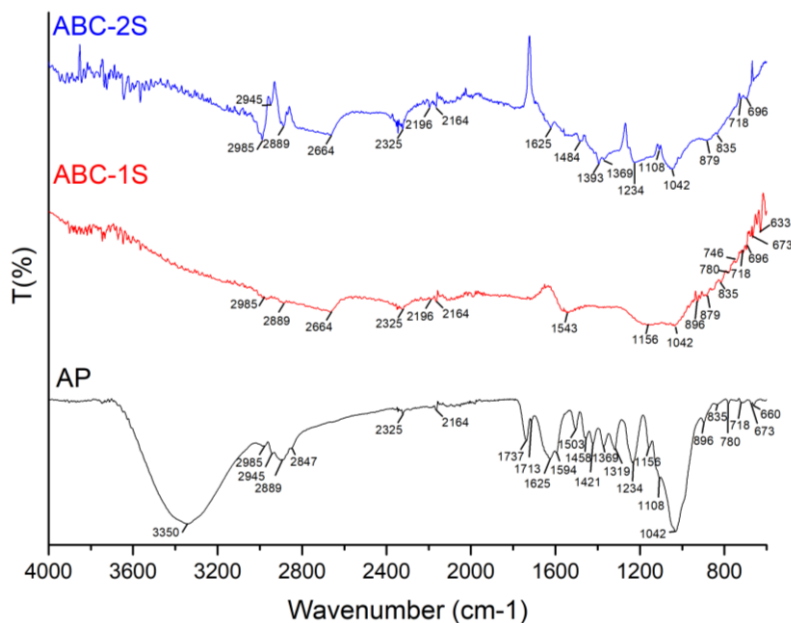


Figure 2: ATR-FTIR spectra of apple pruning (AP), APBC-1S and APBC-2S samples.

As for textural properties of APBC-1S and APBC-2S, the porosity and surface properties are presented in Table 2, while N_2 adsorption-desorption curves at -196°C and pore size distribution curves are shown in Figure 3.

Table 2: Porosity and surface properties (Dubinin-Radushkevich).

Sample	Specific surface (m^2/g)	Micropore volume (cm^3/g)	Average pore width (nm)
APBC-1S	1,297.2	0.569	1.753
APBC-2S	1,176.5	0.503	1.716

APBC-1S sample presented 1.1 times higher specific surface and micropore volume than APBC-2S one, as well as higher average pore width. Both APBC-1S and APBC-2S curves met the type I adsorption isotherm, with a pronounced rise at low relative pressure p/p_0 , indicating micropore filling, followed by a stabilization (Muttakin et al., 2018). Moreover, the presence of a little hysteresis loop indicated the presence of mesopores. APBC-2S sample showed its main porosity in the micropore region (maximum at 0.61 nm), but some important peaks in the range of mesopores appeared (10-14 nm), followed by residual meso-porosity until 50 nm. The cumulative pore volume of APBC-2S sample was close to $0.5 \text{ cm}^3/\text{g}$. Some differences can be observed in the APBC-1S sample; even if its main porosity is located as well in the micropore region (maximum at 0.65 nm), relevant peaks can be seen from 12 to 40 nm (maximum at 12 nm) indicating higher percentage in the mesopore region. This fact could have a relevant influence, as it enhances the availability of the micropores than, in the case of APBC-2S were partially inaccessible.

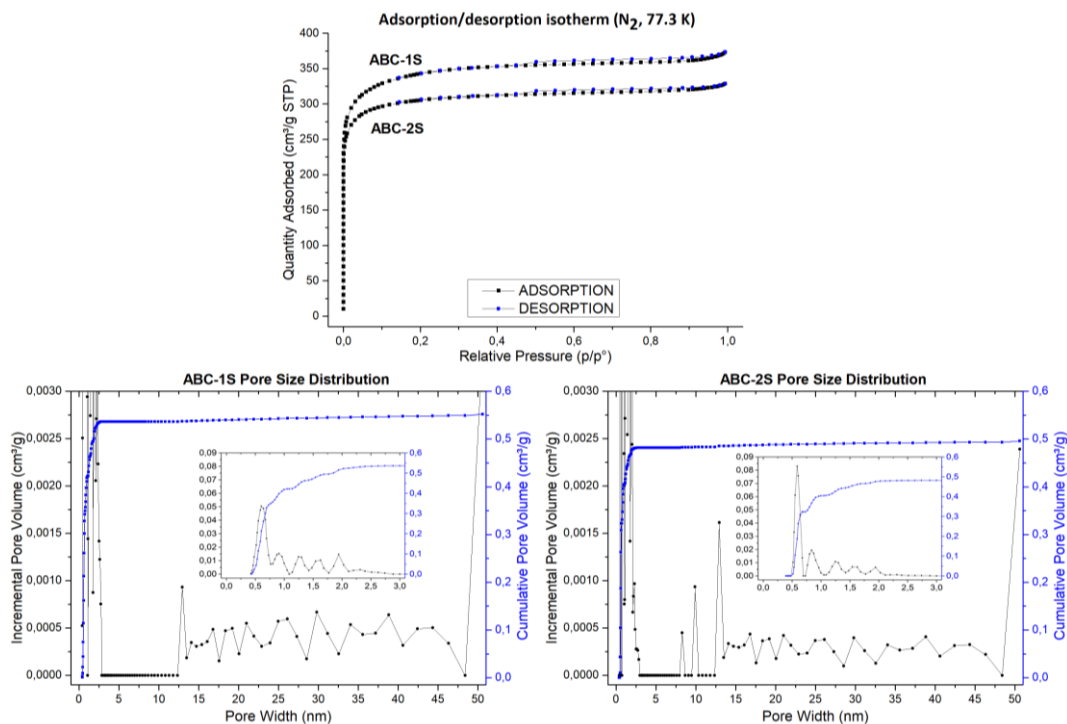


Figure 3: N₂ adsorption-desorption isotherms at -196 °C for APBC-1S (left-up) and APBC-2S (right-up) and calculated (NDFT) pore size distribution curves for APBC-1S (left-down) and APBC-2S (right-down).

3.2 Adsorption results

The performance of both biochars as adsorbents of methylene blue (MB) was measured. This cationic water-soluble dye is extensively used in textiles, plastic, paper, pharmaceuticals, and cosmetics industries (Ashem et al., 2020). Figure 4 shows the results of the adsorption of MB by APBC-1S and APBC-2S samples.

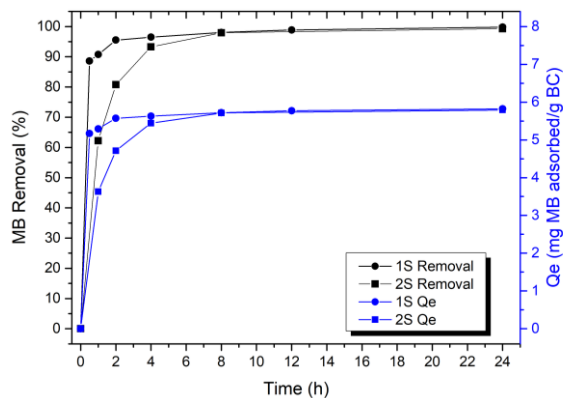


Figure 4: MB adsorption results for APBC-1S and APBC-2S samples.

The biochar obtained by the 1-step procedure reached the best performance, achieving nearly 100% (96%) of MB removal in 4 h, while the adsorbent processed in 2 steps needed 8 h to achieve the same MB removal rate. Thus, the simultaneous use of thermochemical and activation processes enhanced better MB adsorption performance related mainly with the increase of the availability of accessible porosity due to higher pore volume in the mesopore region and the enhancing of accessibility to micropores. The adsorption capacity of both adsorbents was similar (around 6 mg MB adsorbed / g biochar, BC). A complete removal of MB from the original solution was reached by both materials. As the selected initial concentration of the MB solution (35 mg/L) was the one typically found in the dyes industry, that supports the successful performance of both adsorbents at actual conditions.

4. Conclusions

Activated biochars were prepared by two different methods. It was found that the chemical and physical characteristics of the activated carbons obtained varied depending on the conditions of the applied thermochemical and activation processes, influencing the surface area development, pore size distributions and surface chemistry. The biochar prepared in one step (APBC-1S) showed a slightly higher surface area and wider pore size distribution with higher levels of mesoporosity, which improved accessibility of the dye to the available surface area of the adsorbent. This can be seen at the dye adsorption experiments, with removal percentages close to 96% in four hours for APBC-1S, and a complete removal of MB from a solution with a concentration in the range of actual ones of the dyes industry. Furthermore, this opens an opportunity to produce adsorbents by a simultaneous thermochemical and chemical activation processes in one step with no loss of adsorption properties that would be beneficial in terms of time saving and simplicity towards an industrialization of the process.

Acknowledgments

This research has been funded by the Gipuzkoa's Provincial Government under the program "Etorkizuna Eraikiz" 2022/2023.

References

- Antxustegi M., Corro E., Baloch M., Volpe R., Gonzalez Alriols M., 2022, Production of Activated Bio-chars for Wastewater Treatment: Characterization, Activation and Evaluation of the Adsorption Capacity, *Chemical Engineering Transactions*, 92, 547-552.
- Ashem A.H., Saied E., Hasanin M.S., 2020, Green and ecofriendly bio-removal of methylene blue dye from aqueous solution using biologically activated banana peel waste. *Sustain. Chem. Pharm.*, 18, 100333.
- Chen H., Yuan J., Chen G., Zhao X., Wang S., Wang D., Wang Y., 2022. Long-term biochar addition significantly decreases rice rhizosphere available phosphorus and its release risk to the environment. *Biochar*, 4, 1, 54.
- Gallego-Ramírez, C., Chica, E., Rubio- Clemente, A. Coupling of Advanced Oxidation Technologies and Biochar for the Removal of Dyes in Water. *Water* 2022,14,2531.
- Hui T.S., Zaini M.A.A. 2015. Potassium hydroxide activation of activated carbon: a commentary. *Carbon letters* 16, 4, 275-280.
- Jedynak K., Charnas B. 2023. Adsorption properties of biochars obtained by KOH activation. *Adsorption*. <https://doi.org/10.1007/s10450-023-00399-7>.
- Kundu Ch., Biswas S., Thomas B.S., Appadoo D., Duan A., Bhattacharya S., 2023, Evolution of functional group of lignocellulosic biomass and its delignified form during thermal conversion using synchrotron-based THz and laboratory-based in-situ DRIFT spectroscopy, *Fuel*, 348, 128579.
- Liu Y., Weng Z., Han B., Guo Z., Tian H., Tang Y., Cai Y., Yang Z. 2023. Recent studies on the comprehensive application of biochar in multiple environmental fields, *Journal of Cleaner Production*, 421, 138495.
- Lü F., Lu X., Li S., Zhang H., Shao L., He P., 2022, Dozens-fold improvement of biochar redox properties by KOH activation. *Chem. Eng. J.* 429, 132203.
- Luo Z., Yao B., Yang X., Wang L., Xu Z., Yan X., Zhou Y., 2022. Novel insights into the adsorption of organic contaminants by biochar: a review. *Chemosphere* 287, 132113.
- Martelo N., Antxustegi M., Corro E., Baloch M., Volpe R., Gagliano A., Fichera A., Gonzalez Alriols M., 2022, Use of residual lignocellulosic biomass for energetic uses and environmental remediation through pyrolysis, *Energy Storage and Saving*, 1, 3, 129-135.
- Muttakin M., Mitra S., Thu K., Ito K., Saha B.B., 2018, Theoretical framework to evaluate minimum desorption temperature for IUPAC classified adsorption isotherms, *Int. J. Heat Mass Transf.*, 122, 795–805.
- Oginni O., Singh K., Oporto G., Dawson-Andoh B., McDonald L., Sabolsky E. 2019. Influence of one-step and two-step KOH activation on activated carbon characteristics. *Bioresour. Technol. Rep.* 7, 100266–100275.
- Siipola V., Tamminen T., Källi A., Lahti R., Romar H., Rasa K., Keskinen R., Hyväluoma J., Hannula M., Wikberg H., 2018. Effects of biomass type, carbonization process, and activation method on the properties of bio-based activated carbons" *BioRes.* 13 (3), 5976-6002.
- Sun Y., Wang T., 2023, Application of Biochar, Adsorbent and Nanomaterials in Wastewater Treatment. *Water*, 15, 1320.
- Wang, T., Camps-Arbestain, M., Hedley, M., 2013. Predicting C aromaticity of biochars based on their elemental composition. *Organic Geochemistry* 62, 1-6.
- Wiedemeier D.B., Abiven S., Hockaday W.C., Keiluweit M., Kleber M., Masiello C.A., McBeath A.V., Nico P.S., Pyle L.A., Schneider M.P.W., Smernik R.J., Wiesenberger G.L.B., Schmidt M.W.I., 2015, Aromaticity and degree of aromatic condensation of char, *Organic Geochemistry*, 78, 135-143.